

Final Report

**Post Rim Fire Assessment of Fuel Consumption and Mortality in the Yosemite
Forest Dynamics Plot**

**Final Report to the National Park Service
Cooperative Agreement**

Cooperative Agreement H1200090005

Task Agreement P14AC00197
CPCESU

Task Agreement P14AC00122
RMCESU

James A. Lutz, Andrew J. Larson, Kendal M. L. Becker, Tucker J. Furniss, Erika
M. Blomdahl, Sara J. Germain, and Mark E. Swanson

April 8, 2016

Final Report

National Park Service Award Task Agreements P14AC00197 and P14AC00122 for Cooperative Agreement, H1200090005, (USUCP-72, UMT-296) Post Rim Fire Assessment of Fuel Consumption and Mortality in the Yosemite Forest Dynamics Plot

James A. Lutz, Principal Investigator
Andrew J. Larson, Co-Principal Investigator

Overview: The Yosemite Forest Dynamics Plot (YFDP) is a 25.6 ha research site approximately 1 km north of the Crane Flat Lookout. The YFDP was established in 2008-2009 and has been monitored annually since that time. At plot establishment, it was expected that the site would be burned by a prescribed fire. Therefore, considerable pre-fire fuels information was collected along with the standard demography data specified in the Smithsonian Center for Tropical Forest Science ForestGEO protocols. The Rim Fire event of August-September 2013 resulted in the burning of the YFDP. As part of a management-ignited backfire, the north side of the Crane Flat Helitack hill was ignited from the parking lot, and the fire was allowed to back downslope with no active management. Portions of the YFDP were burned by the backing fire, and other portions were burned the following day as the fire burned upslope.

Previous research in the YFDP has documented field methods (Lutz et al. 2012) and provided some insight into fuel strata (e.g., cones; Gabrielson et al. 2012), shrub communities (Lutz et al. 2014), woody plant diversity and phylogenies (Erickson et al. 2014), large-diameter trees (Lutz et al. 2012; 2013), and the historical fire regime and pre-suppression forest conditions (Barth et al. 2015). Data from the YFDP has also been used in global comparisons of forest structure (Chisholm et al. 2013, Réjou-Méchain et al. 2014, Anderson-Teixeira et al. 2015).

Subsequent to the Rim Fire of 2013, the value of a matched set of pre-fire and post-fire data on forest conditions in the lower montane forests of Yosemite National Park became apparent, and this cooperative study was funded to acquire baseline data that could be used by park managers to better understand the consequences of the resumption of fire following a century of fire exclusion (Lutz 2015).

Task 1: *Construct full pre-fire and post-fire datasets for all subsequent fire effects and demographic analysis.*

Our pre-fire sampling in 2009-2013, plus our post-fire sampling in 2014, combined with additional field surveys in 2015 to confirm and correct data, resulted in baseline pre-fire and post-fire data sets detailed below.

Task 2: *Assess mortality of all trees in the YFDP and assess status of snags.*

Tree mortality was assessed in 2014. Tree mortality was also assessed in 2015, and we will continue to monitor post-fire mortality as part of our long-term program (outside the scope of this project). Immediate tree mortality was 70% of tree stems, but mortality of large-diameter trees was under 5% (Table 1). The population of snags increased commensurate with the high number of tree mortalities (Table 2). However, at diameters (diameter at breast height; 1.37 m

above the pre-fire ground surface) most appropriate for cavity dwelling vertebrates (DBH >60 cm), the number of snags declined, with increases in snags due to tree mortality not quite equaling the number of pre-fire snags consumed by fire or fallen.

Task 3: *Determine scorch assessment on trees and snags in the YFDP (scorch height, percent scorch, and char height).*

Logistic regressions were performed in the form of Equation 1. Canopy scorch percentage was an important predictor of immediate post-fire mortality (Fig. 1). Bole scorch height was not as predictive of immediate post-fire mortality as canopy scorch, but bole scorch height and the interaction of bole scorch height and DBH were significant (Table 3). Bole scorch may be a more important factor, along with canopy scorch percentage, in delayed fire mortality. Bole scorch height is confounded with tree height – taller trees can have higher scorch heights while their canopy remains relatively unaffected. In the future, it may be possible to improve this preliminary model with terms representing local tree neighborhood and landscape position.

$$\text{Eq. 1: } \text{Logit}(\text{Mortality}) = A + B \times (\text{Bole Scorch}) + C \times (\text{Canopy Scorch}) + D \times (\text{DBH}) + E \times (\text{Bole Scorch} \times \text{DBH})$$

Task 4: *Measure surface fuel consumption along fuels transects between monuments to determine magnitude and heterogeneity of fuel consumption.*

Our field measurements of fuel consumption examined standard fuels (litter, duff, 1-hour, 10-hour, 100-hour fuels), and also more explicit tallying of larger fuels (1000-hour, and above). We also examined shrub biomass and consumption. Wood intercepts along the 2,240 m of fuel transects followed Weibull distributions both pre-fire (2011) and post-fire (2014) (Fig. 2). Pre-fire Weibull parameters were 1.27 ± 0.06 for shape, and 13.26 ± 0.68 for scale. Post-fire Weibull parameters were 1.21 ± 0.06 for shape and 31.10 ± 2.04 for scale (Fig. 2). In general, 1-hour (Fig. 3), 10-hour (Fig. 4), and 100-hour fuels (Fig. 5) were reduced by a factor of two or more, with post-fire new additions comprising the majority of these pools in the 2014 measurement period. Net reduction of 100-hour fuels was especially notable, as was reduction in the 7.62 – 30 cm range of down woody debris. Post-fire mortality and small-diameter snag fragmentation is expected to increase levels in these pools, however. The equation predicting forest floor biomass from fuel bed depth (cm) is from Stephens and Whitney (2001).

Larger fuels decreased by a factor of two (Fig. 6), but litter and duff decreased 90% (Fig. 7). Total surface fuel loading (litter, duff, and all down woody material) decreased 90% as calculated by the transect method (Fig. 8).

In addition to the standard measurements of fuel along transects (above), we also explicitly mapped woody debris having any dimension ≥ 50 cm diameter (Tables 4 5; Fig. 10). Lengths of debris were measured as were diameters of both ends pre-fire and post-fire. Differing from the statistical approach used with the intercept method, this permits a more precise calculation of wood volume.

We also mapped shrub patches to analyze consumption (Fig. 9) and mapped small-scale unburned patches (Fig. 11). Unburned patches $\geq 1 \text{ m}^2$ were mapped to examine whether these small-scale refugia might have different post-fire developmental trajectories than areas that were

burned. There were a total of 685 unburned patches totaling 12,562 m² (Fig. 11). Unburned areas occurred in all landscape positions, but were more prevalent in the mesic draws. The largest single unburned patch was in the very wet *Cornus sericea* patch in the southwest corner of the YFDP.

Table 1. Mortalities in the Yosemite Forest Dynamics Plot, 2011-2015. The plot burned September 2-3, 2013, after the 2013 measurement. The 2014 post-fire sampling was done in May 2014 to separate immediate fire mortalities (2014 column, 9 months post-fire) from delayed mortalities.

	2010 Initial Population	Mortalities				Remaining as of 6/2015	
		2011	2012	2013	2014	2015	
By species		Pre-fire			Post-fire		
<i>Abies concolor</i>	24,537	441	376	415	17,402	1,963	4,627
<i>Pinus lambertiana</i>	4,800	78	110	138	2,948	263	1,404
<i>Cornus nuttallii</i>	2,361	9	18	34	2,072	125	524
<i>Calocedrus decurrens</i>	1,600	5	8	4	1,044	96	495
<i>Quercus kelloggii</i>	1,117	13	20	17	700	70	346
Other species	164	2	4	8	153	9	12
Total	34,579	548	536	616	24,319	2,526	7,408
By diameter class							
1 cm ≤ dbh < 10 cm	21,157	341	344	467	18,833	685	1,212
10 cm ≤ dbh < 30 cm	9,722	178	144	120	5,120	1,544	2,974
30 cm ≤ dbh < 60 cm	2,349	18	29	19	317	252	1,944
60 cm ≤ dbh < 90 cm	710	6	8	6	25	28	682
dbh ≥ 90 cm	641	5	11	4	24	17	596
Total	34,579	548	536	616	24,319	2,526	7,408

Table 2. Snag population in the Yosemite Forest Dynamics Plot, 2010-2015. Snags are dead standing trees ≥10 cm DBH. Changes in snag abundance reflect the net effect of tree mortality and snags falling to the ground.

	2010 Initial Population						
		2011	2012	2013	2014	2015	
By species		Pre-fire			Post-fire		
<i>Abies concolor</i>	1,989	2,051	2,082	2,093	5,320	6,365	
<i>Pinus lambertiana</i>	535	528	526	544	945	1,070	
<i>Cornus nuttallii</i>	1	1	2	3	184	190	
<i>Calocedrus decurrens</i>	48	49	48	49	263	306	
<i>Quercus kelloggii</i>	131	129	133	137	461	459	
Other species	8	8	9	8	5	6	
Total	2,712	2,766	2,800	2,834	7,178	8,396	
By diameter class							
10 cm ≤ dbh < 30 cm	1,794	1,844	1,863	1,889	6,142	7,184	
30 cm ≤ dbh < 60 cm	482	484	499	502	628	798	
60 cm ≤ dbh < 90 cm	169	173	176	179	164	173	
dbh ≥ 90 cm	267	265	262	264	244	241	
Total	2,712	2,766	2,800	2,834	7,178	8,396	

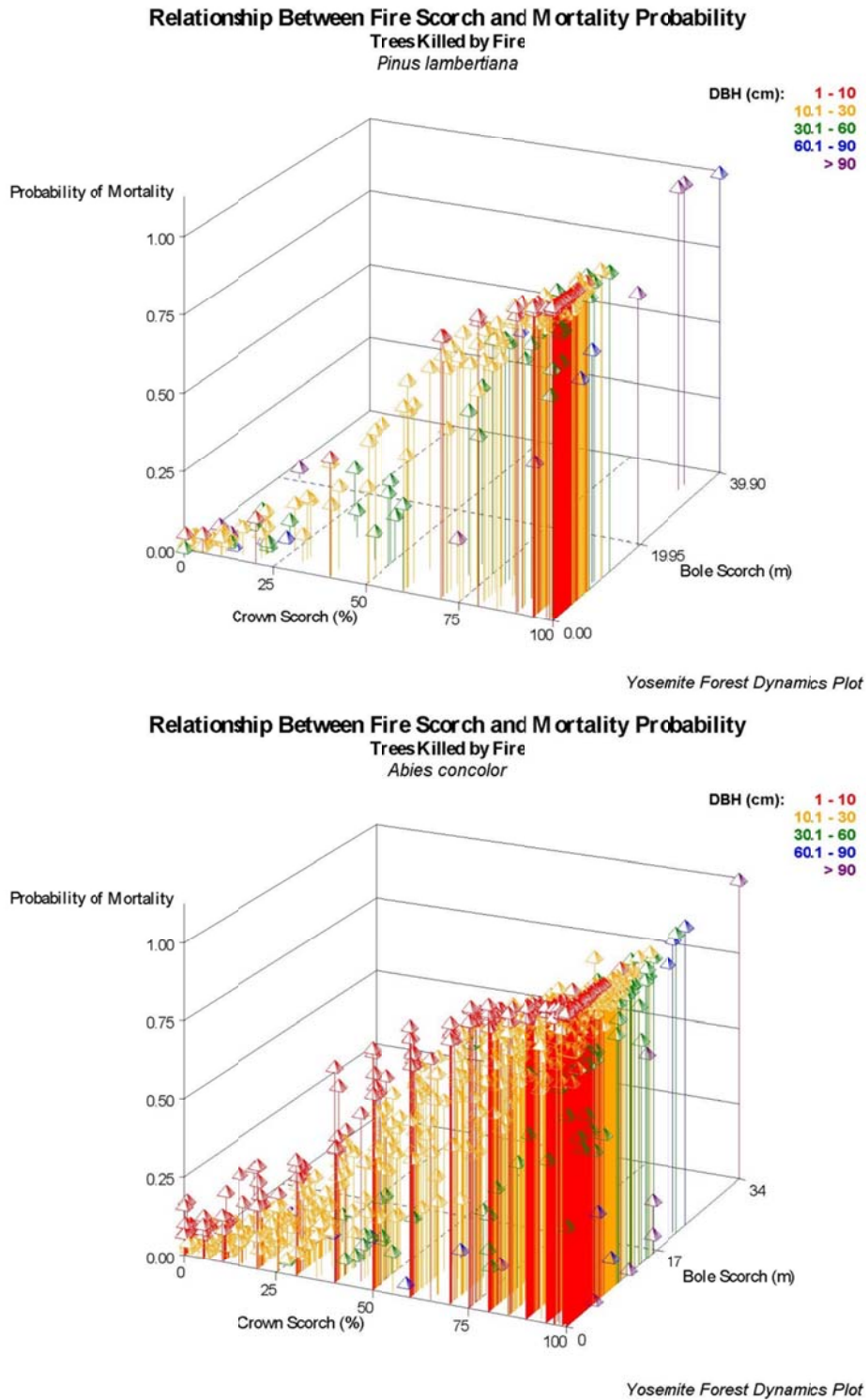


Figure 1a. Probability of immediate post-fire mortality for *Abies concolor* and *Pinus lambertiana* in the Yosemite Forest Dynamics Plot.

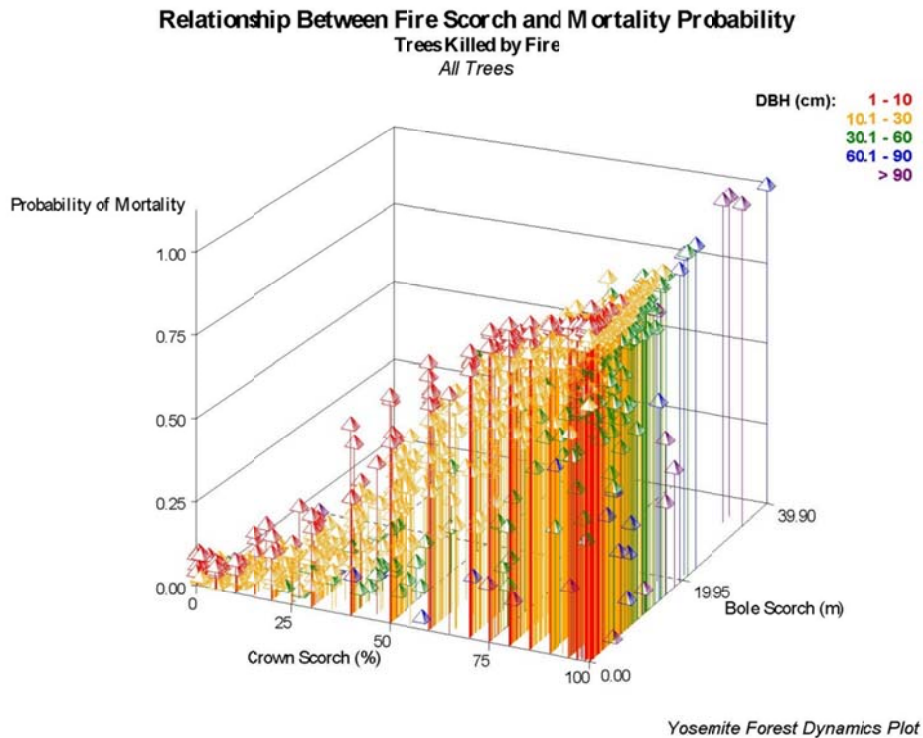


Figure 1b. Probability of immediate post-fire mortality for all trees in the Yosemite Forest Dynamics Plot.

Table 3. Logistic regression parameters for probability of mortality for *Abies concolor*, *Pinus lambertiana*, and all trees in the Yosemite Forest Dynamics Plot.

<i>Abies concolor</i> , AUC = 0.977, Pseudo R ² = 0.78				
Parameter	Parameter Estimate	Point Estimate	P-value	
Intercept	-1.3458	0.260	< 0.0001	
Bole Scorch	0.0607	1.063	0.0119	
Crown Scorch	0.0593	1.061	< 0.0001	
DBH	-0.1379	0.871	< 0.0001	
Bole Scorch*DBH	0.00436	1.004	< 0.0001	
<i>Pinus lambertiana</i> , AUC = 0.989, Pseudo R ² = 0.87				
Parameter	Parameter Estimate	Point Estimate	P-value	
Intercept	-2.2872	0.102	< 0.0001	
Bole Scorch	0.0554	1.057	0.2458	
Crown Scorch	0.0616	1.064	< 0.0001	
DBH	-0.0744	0.928	< 0.0001	
Bole Scorch*DBH	0.00296	1.003	< 0.0001	
All trees, AUC = 0.977, Pseudo R ² = 0.80				
Parameter	Parameter Estimate	Point Estimate	P-value	
Intercept	-1.9895	0.137	< 0.0001	
Bole Scorch	0.0591	1.061	0.0015	
Crown Scorch	0.0619	1.064	< 0.0001	

DBH	-0.1170	0.890	< 0.0001
Bole Scorch*DBH	0.00414	1.004	< 0.0001

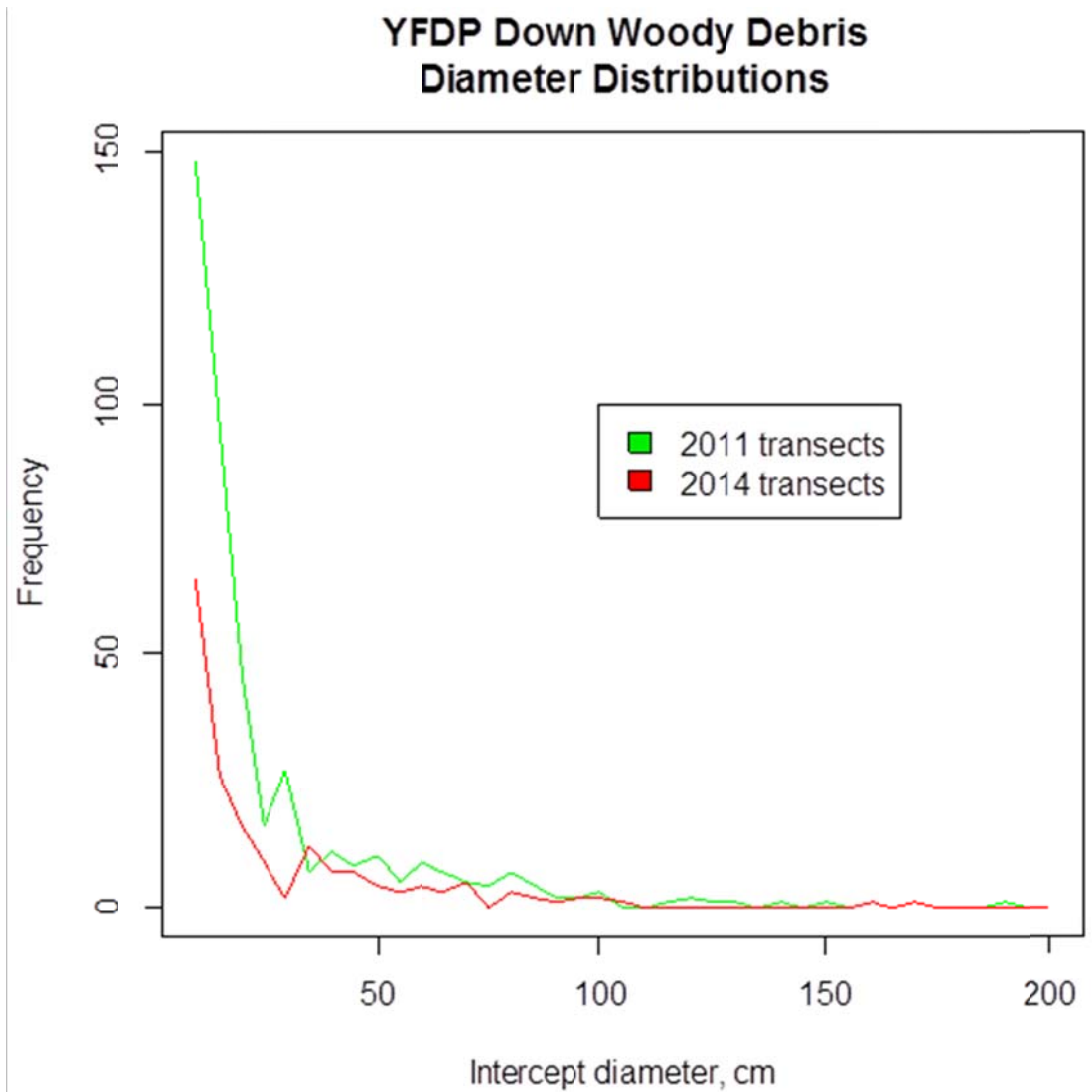


Figure 2. Fuel transect intercepts of down woody debris (>7.6 cm in diameter). At diameters below ~30 cm fire consumption was greater than new woody debris produced by fire.

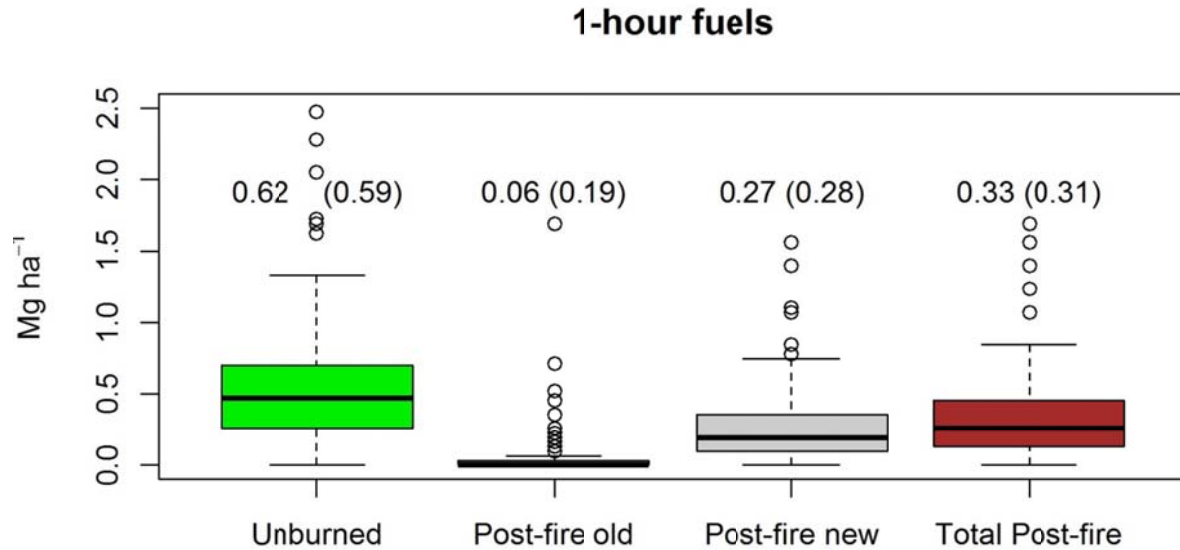


Figure 3. Calculated biomass of 1-hour woody fuels (not including conifer needles; $0 < \text{diameter} < 0.635 \text{ cm}$) from short (2 m) Brown transects ($n=112$ for both 2011 and 2014) placed within first 2 m of each 20-m line-intercept transect. ‘Post-fire old’ represents material that persisted as ground fuels through the 2013 fire event, while ‘post-fire new’ represents material that became ground fuel following the fire event. ‘Total post-fire’ is the sum of the latter classes.

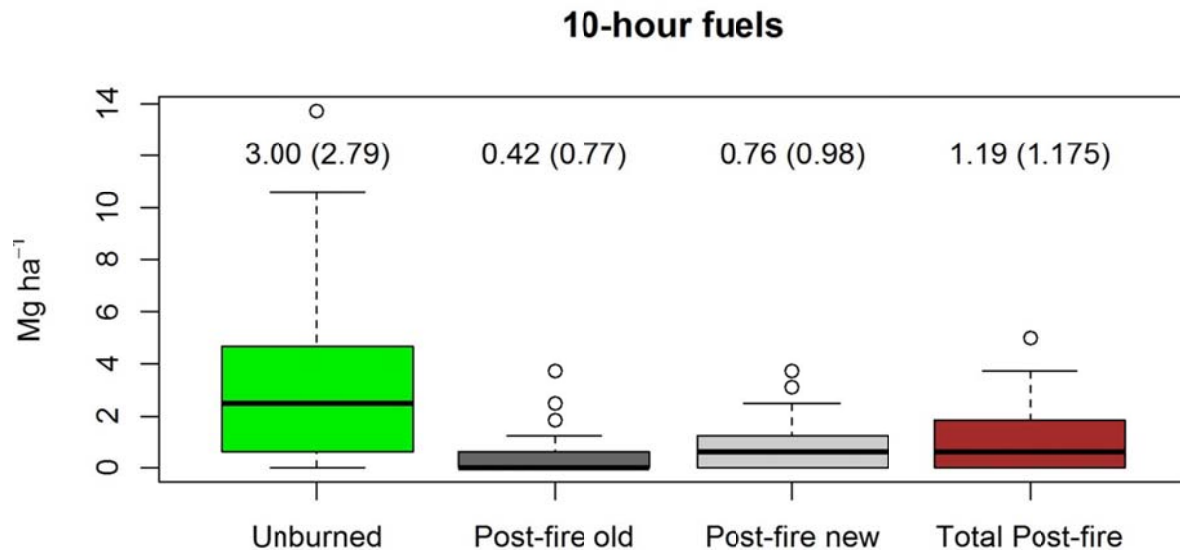


Figure 4. Calculated biomass of 10-hour woody fuels ($0.635 \leq \text{diameter} < 2.54 \text{ cm}$) from short (2 m) Brown transects placed within first 2 m ($n=112$ for both 2011 and 2014) of each 20-m line-intercept transect. ‘Post-fire old’ represents material that persisted as ground fuels through the 2013 fire event, while ‘post-fire new’ represents material that became ground fuel following the fire event. ‘Total post-fire’ is the sum of the latter classes.

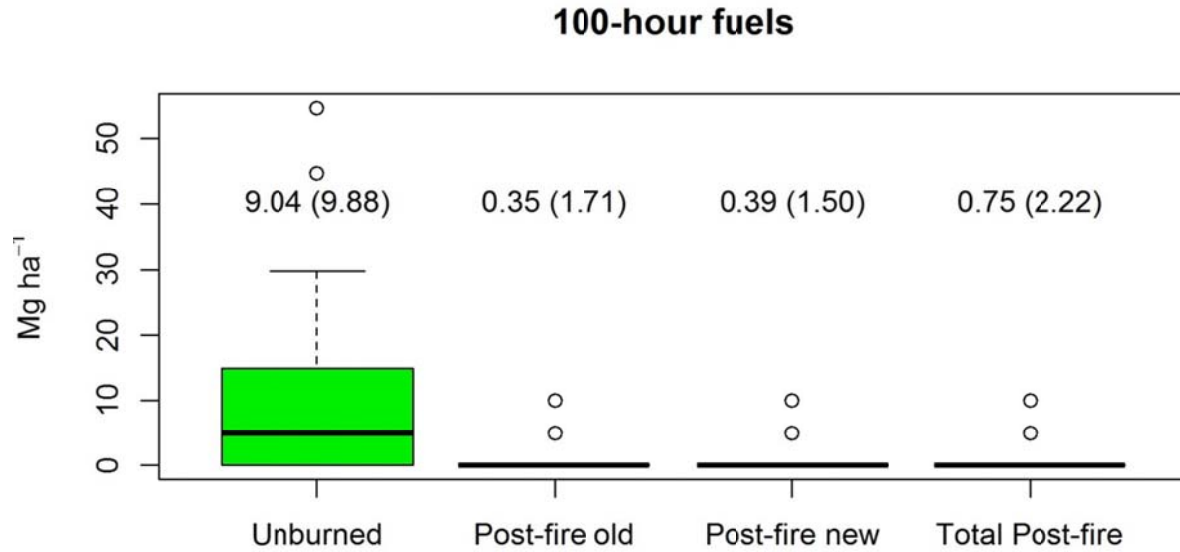


Figure 5. Calculated biomass of 100-hour woody fuels ($2.54 \leq \text{diameter} < 7.62 \text{ cm}$) from short (2 m) Brown transects ($n=112$ for both 2011 and 2014) placed within first 2 m of each 20-m line-intercept transect. ‘Post-fire old’ represents material that persisted as ground fuels through the 2013 fire event, while ‘post-fire new’ represents material that became ground fuel following the fire event. ‘Total post-fire’ is the sum of the latter classes.

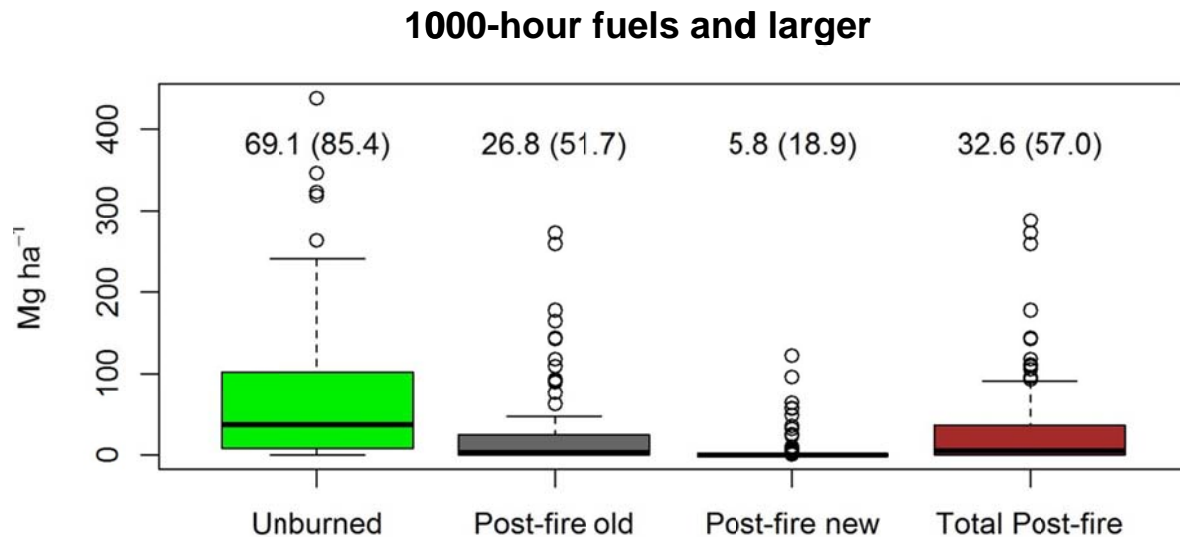


Figure 6. Calculated biomass of large woody fuels ($> 7.62 \text{ cm}$ intercept diameter) in 2011 (unburned), and post-fire (2014). ‘Post-fire old’ represents material that persisted as ground fuels through the 2013 fire event, while ‘post-fire new’ represents material that became ground fuel following the fire event. ‘Total post-fire’ is the sum of the latter classes. Species-specific decay class bulk densities were used to convert estimated volumes to per-hectare biomass estimates.

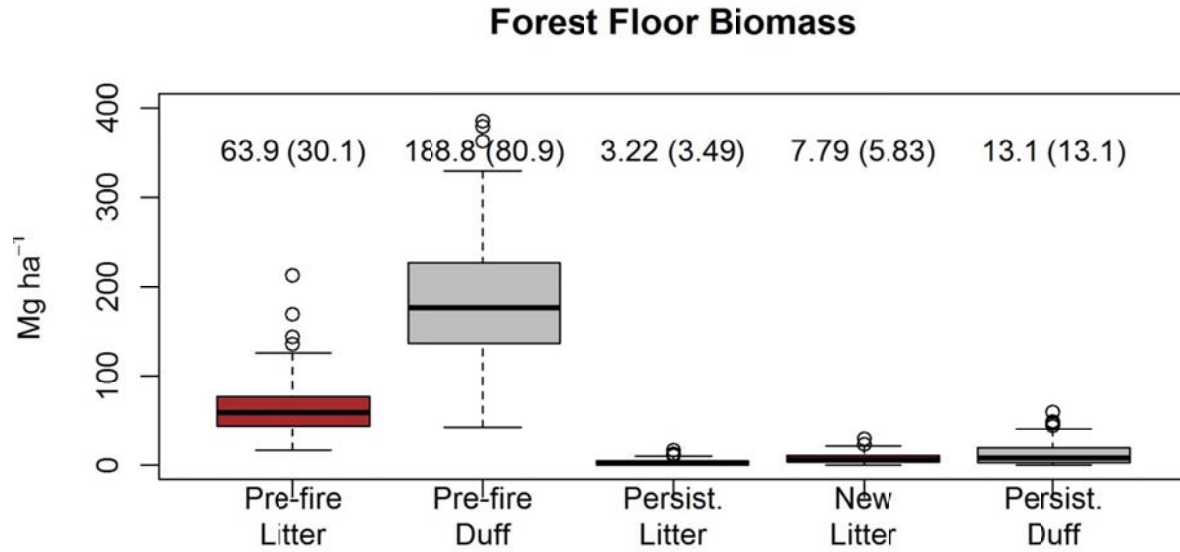


Figure 7. Forest floor (litter and duff) estimated biomass from discrete depth sampling points along 20-m transects (n=112, with 4 and 10 subsample points for the 2011 and 2014 data, respectively). ‘Post-fire old’ represents material that persisted as ground fuels through the 2013 fire event, while ‘post-fire new’ represents material that became ground fuel following the fire event. ‘Total post-fire’ is the sum of the latter classes, calculated by the methods in Stephens et al. (2004).

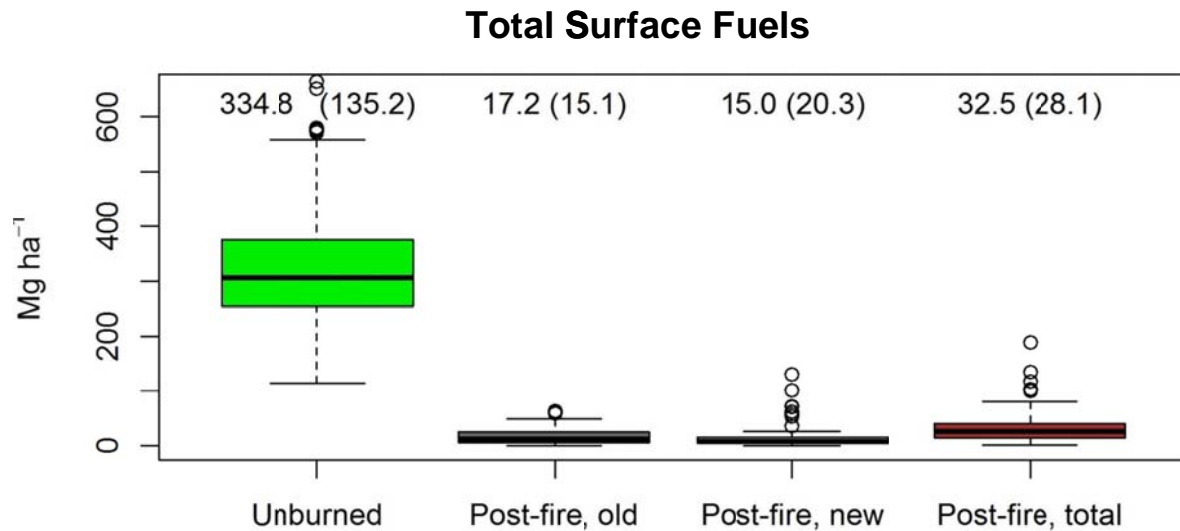


Figure 8. Total biomass of surface fuels from all strata calculated using the intercept method along fuel transects. Post-fire surface fuel loading was <10% of pre-fire surface fuel loading.

Table 3. Inventory of explicitly mapped pre-fire coarse woody debris ≥ 50 cm diameter in the Yosemite Forest Dynamics Plot (25.6 ha). Pieces were assigned to size classes based on maximum diameter.

Pre-fire	<i>Abies concolor</i>	<i>Calocedrus decurrens</i>	<i>Pinus lambertiana</i>	<i>Quercus kelloggii</i>	Unknown	Total
50-60 cm						
No. pieces	151	18	120	1	15	305
Vol. (m ³)	89.93	6.75	68.29	0.73	5.72	171.42
60-90 cm						
No. pieces	273	57	270	–	68	668
Vol. (m ³)	349.59	79.07	360.26	–	61.63	850.56
>90 cm						
No. pieces	50	36	258	–	36	380
Vol. (m ³)	257.09	175.30	2101.83	–	80.83	2615.06
Total						
No. pieces	474	111	648	1	119	1353
Vol. (m ³)	696.60	261.13	2530.38	0.73	148.18	3637.03

Table 4. Inventory of explicitly mapped post-fire coarse woody debris in the Yosemite Forest Dynamics Plot (25.6 ha), including all detectable pieces that were ≥ 50 cm diameter pre-fire and newly fallen pieces ≥ 50 cm diameter. Pieces were assigned to size classes based on maximum diameter.

Post-fire	<i>Abies concolor</i>	<i>Calocedrus decurrens</i>	<i>Pinus lambertiana</i>	<i>Quercus kelloggii</i>	Unknown	Total
<10 cm						
No. pieces	2	–	3	–	1	6
Vol. (m ³)	0.01	–	0.02	–	0.01	0.04
10-30 cm						
No. pieces	114	25	94	1	23	257
Vol. (m ³)	9.11	1.39	9.26	0.304	1.30	21.36
30-50 cm						
No. pieces	160	42	221	–	33	456
Vol. (m ³)	53.60	16.03	90.09	–	7.54	167.26
50-60 cm						
No. pieces	66	21	105	–	5	197
Vol. (m ³)	63.08	16.63	91.19	–	2.13	173.02
60-90 cm						
No. pieces	67	37	199	–	10	313
Vol. (m ³)	155.10	77.82	589.56	–	10.19	832.67
>90 cm						
No. pieces	5	13	128	–	1	147
Vol. (m ³)	45.01	68.54	1384.36	–	2.46	1500.36
Total						
No. pieces	414	138	750	1	73	1376
Vol. (m ³)	325.90	180.42	2164.48	0.304	23.63	2694.73

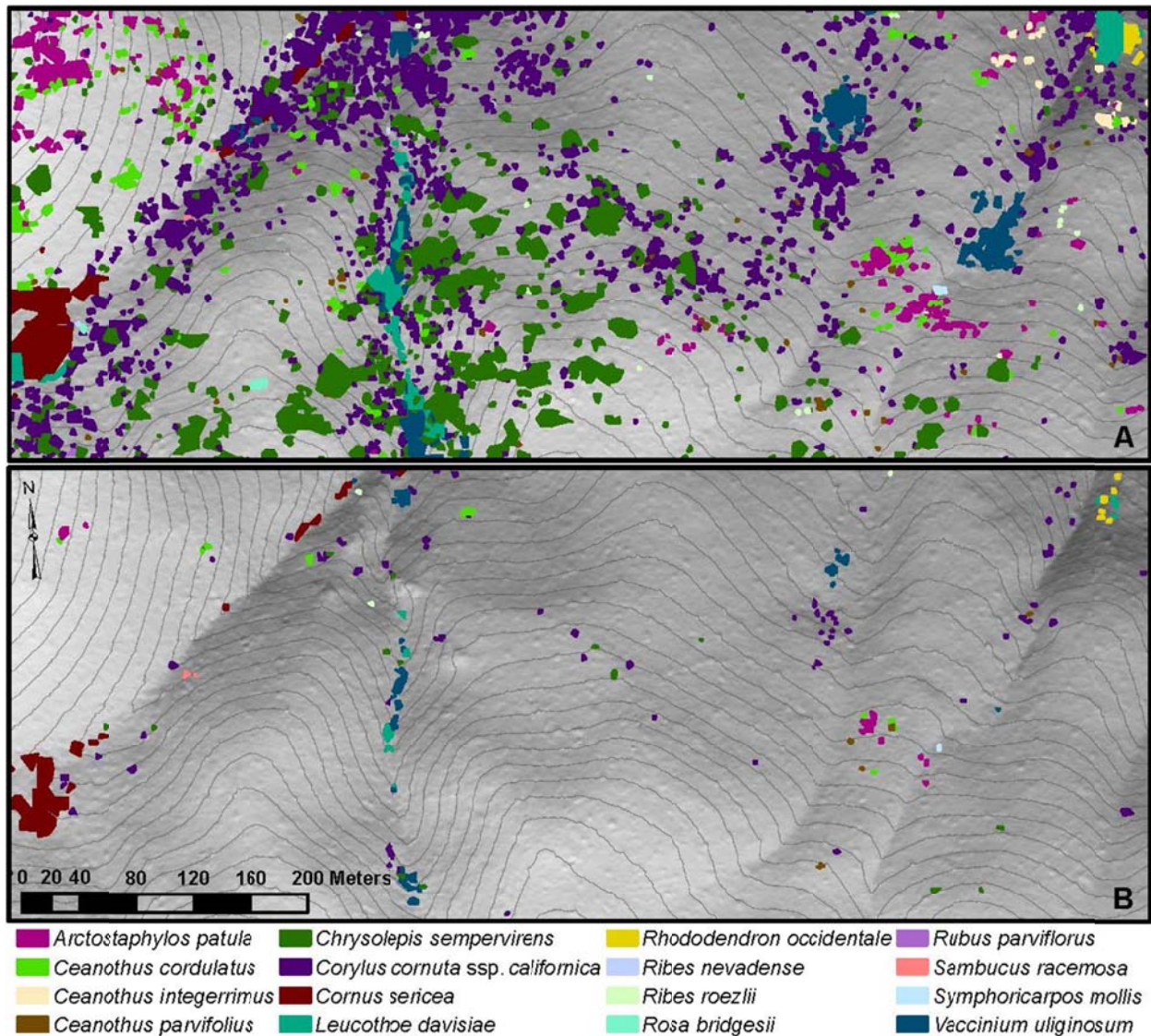


Figure 9. Shrub consumption by fire in the Yosemite Forest Dynamics Plot. Pre-fire patches (A) covered 15.1% of the plot, with the area influenced by shrub burning (1 m buffer around patches) covering 25.2% of the plot. Although most of the shrub patches that remained post-fire (B) were located in moist swales, shrub patches persisted in all landscape positions. Even when shrub patches were consumed by fire or top-killed, a majority were observed with new sprouts in 2014 and 2015. As the shrubs continue to recruit into larger diameter classes, they will be mapped and tagged according to the tree protocol.

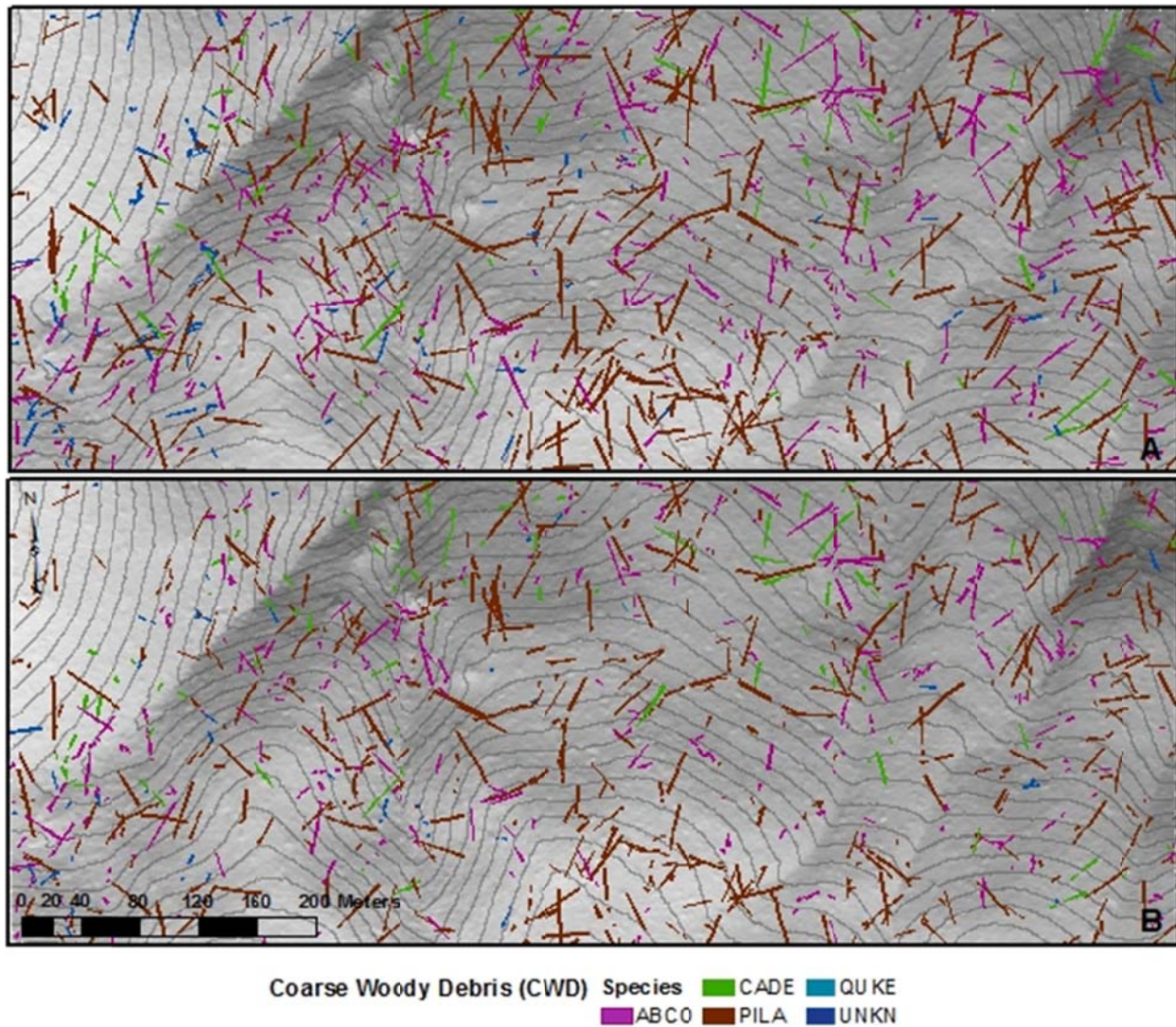


Figure 10. Coarse woody debris in the Yosemite Forest Dynamics Plot. Pre-fire (A) and post-fire (B) coarse woody debris include all pieces that were ≥ 50 cm diameter at the large end pre-fire and newly fallen coarse woody debris ≥ 50 cm diameter at the large end.

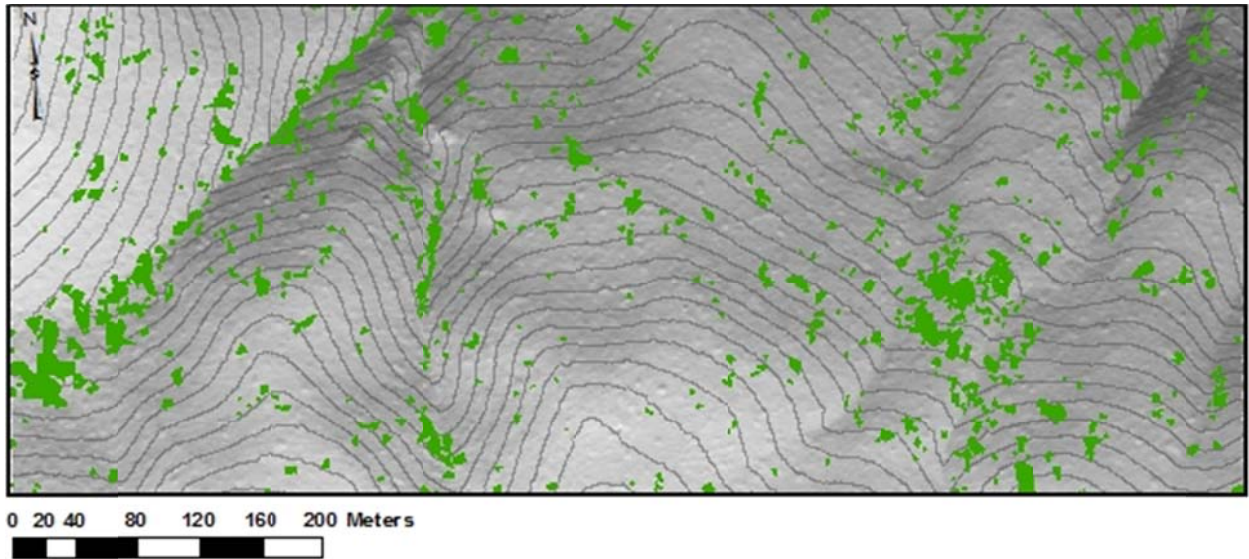


Figure 11. Unburned patches $\geq 1 \text{ m}^2$ within the Yosemite Forest Dynamics Plot.

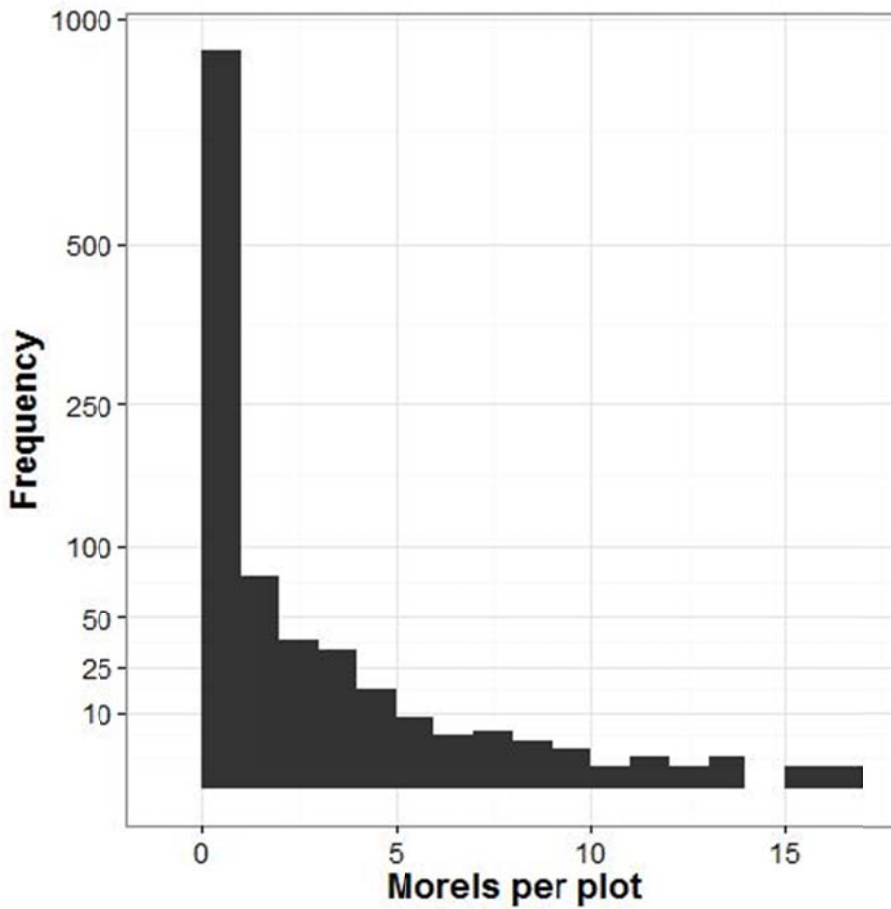


Figure 12. Frequency distribution of morel mushroom counts sampled in 3.14 m^2 plots located along the fuels transects within the YFDP.

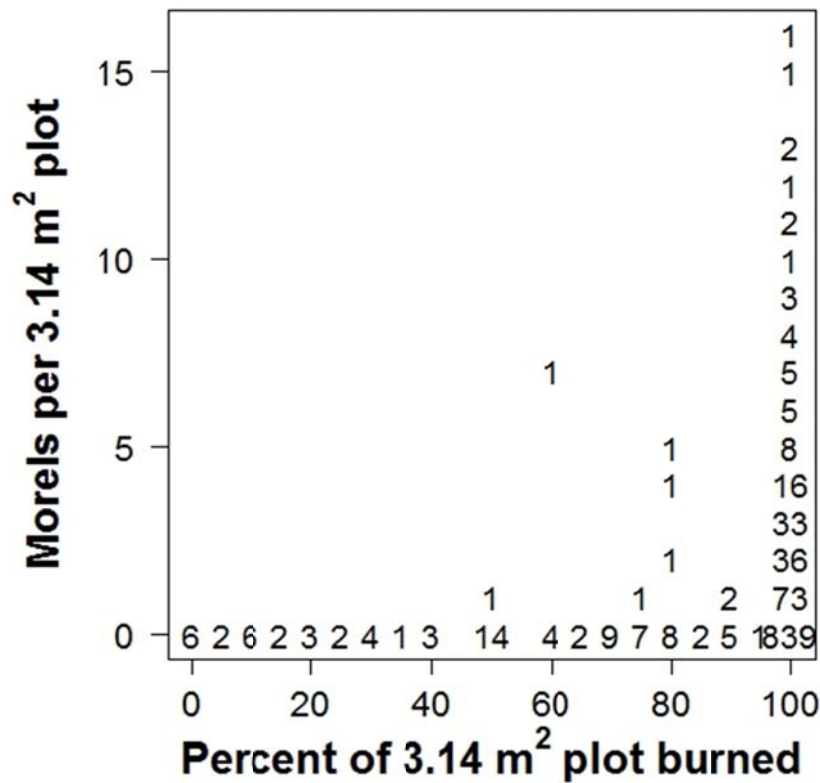


Figure 13. Relationship between the count of morel mushrooms per plot and the percentage of plot surface area the burned. Graph symbols are the number of plots observed for each percent burned – morel count combination.

We surveyed the occurrence of morel (*Morchella*) ascocarps (i.e., mushrooms) in n=1119 circular 1 m radius plots located along the 2,240 m of fuel transects. We counted a total of 595 morel ascocarps in the 1119 plots. These mushrooms occurred in 17.8% of plots, the remaining 82.2% of plots did not contain morels. The maximum count of morels within a single 3.14 m² plot was 16 individuals, which occurred once (Figure 12). We estimated a mean standing crop of 1693 morels ha⁻¹ (SE = 155 morels ha⁻¹). Morels did not occur in plots in which <50% of the surface was burned; the overwhelming majority of morel-occupied plots were 100% burned (Figure 13). This appears to be the first estimate of post-fire morel mushroom productivity for Sierra Nevada mixed-conifer forest, and one of only two estimates of post-fire morel productivity estimates in the western contiguous United States.

Task 5: *Re-read and replace damaged dendrometers to measure post-fire tree growth.*

Dendrometers were reset, and we continue to read them 2-3 times per year. We continue to measure dendrometers on trees that have died until the bark separates from the wood. As of August 2015, there are 348 dendrometers on living trees within the YFDP.

Task 6: *Enter and conduct QA/QC on data entered into database.*

Due to the volume and variability of the data, QA/QC took much longer than planned. We conducted a field check on questionable items in 2015, and believe that the datasets now have a very high accuracy level for detailed analysis.

Task 7: *Analyze data to report on post-fire mortality of trees of different size classes, scorch and char associated with fire-killed trees, fate of snags and large downed wood, and surface fuel consumption.*

Basic summary and analysis is provided in Tables 1-5 and Figures 1-13 (above).

Task 8: *Access to data and report.*

Data are available to Park managers or collaborators for *bona fide* research or management objectives. Data presented in this report have not yet been peer-reviewed. The project team are currently preparing the following peer review publications for submission in Q2 2016.

Lutz, J. A., T. J. Furniss, S. J. Germain, K. M. L. Becker, E. Blomdahl, S. A. Jeronimo, J. A. Freund, M. E. Swanson, and A. J. Larson. Submitted. Shrub consumption and community change by reintroduced fire in Yosemite National Park, California, USA. *Canadian Journal of Forest Research*.

Larson, A. J., C. A. Cansler, S. G. Cowdery, S. Hiebert, T. J. Furniss, M. E. Swanson, and J. A. Lutz. In preparation. Morel mushroom production, spatial autocorrelation, and harvest sustainability following fire in a Sierra Nevada mixed-conifer forest. *Forest Ecology and Management*.

Swanson, M. E., R. Burke, C. A. Cansler, A. J. Larson, J. A. Freund, and J. A. Lutz. In preparation. Forest floor and woody fuels characteristics in an old-growth Sierra Nevada mixed-conifer forest: effects of low-severity fire, forest structure, and microtopography. *Forest Ecology and Management*.

We are also in early stages of preparing manuscripts on the subject of snag demography, spatial aspects of tree mortality, and the correlations between tree mortality and Landsat-derived spectral indices. On April 8, 2016 we received funding from the Joint Fire Science Program to pursue these avenues of research.

References

Anderson-Teixeira, K. J., S. J. Davies, A. C. Bennett, E. B. Gonzalez-Akre, H. C. Muller-Landau, S. J. Wright, K. Abu Salim, J. L. Baltzer, Y. Bassett, N. A. Bourg, E. N. Broadbent, W. Y. Brockelman, S. Bunyavejchewin, D. F. R. P. Burslem, N. Butt, M. Cao, D. Cardenas, K. Clay, R. S. Condit, M. Detto, X. Du, A. Duque, D. L. Erikson, C. E.N. Ewango, C. D. Fletcher, G.

- S. Gilbert, N. Gunatilleke, S. Gunatilleke, Z. Hao, W. H. Hargrove, T. B. Hart, B. Hao, F. He, F. M. Hoffman, R. Howe, S. P. Hubbell, P. A. Jansen, M. Jiang, M. Kanzaki, D. Kenfack, M. F. Kinnaird, J. Kumar, A. J. Larson, Y. Li, X. Li, S. Liu, S. K.Y. Lum, J. A. Lutz, K. Ma, D. Maddalena, J. R. Makana, Y. Malhi, T. Marthews, S. McMahon, W. J. McShea, H. Memiaghe, X. Mi, T. Mizuno, J. A. Myers, V. Novotny, A. A. de Oliveira, D. Orwig, R. Ostertag, J. den Ouden, G. Parker, R. Phillips, A. Rahman, K. Sri-ngernyuang, R. Sukumar, I. F. Sun, W. Sungpalee, S. Tan, S. C. Thomas, D. Thomas, J. Thompson, B. L. Turner, M. Uriarte, R. Valencia, M. I. Vallejo, A. Vicentini, T. VrÅjka, X. Wang, G. Weiblen, A. Wolf, H. Xu, W. Xugao, S. Yap, and J. Zimmwerman. 2015. CTFS-ForestGEO: A worldwide network monitoring forests in an era of global change. *Global Change Biology* 21(2): 528-549. doi: <http://dx.doi.org/10.1111/gcb.12712>
- Barth, M. A. F., A. J. Larson, and J. A. Lutz. 2015. Use of a forest reconstruction model to assess changes to Sierra Nevada mixed-conifer forest during the fire suppression era. *Forest Ecology and Management* 354: 104-118. doi: <http://dx.doi.org/10.1016/j.foreco.2015.06.030>
- Chisholm, R. A., H. C. Muller-Landau, K. Abd. Rahman, D. P. Bebbler, Y. Bin, S. A. Bohlman, N. A. Bourg, J. Brinks, N. Brokaw, S. Bunyavejchewin, N. Butt, H. Cao, M. Cao, D. Cárdenas, L. W. Chang, J. M. Chiang, G. Chuyong, R. Condit, H. S. Dattaraja, S. Davies, A. Duque, C. Fletcher, C. V. S. Gunatilleke, I. A. U. N. Gunatilleke, Z. Hao, R. D. Harrison, R. Howe, C. F. Hsieh, S. Hubbell, A. Itoh, D. Kenfack, S. Kiratiprayoon, A. J. Larson, J. Lian, D. Lin, H. Liu, J. A. Lutz, K. Ma, Y. Malhi, S. McMahon, W. McShea, M. Meegaskumbura, S. M. Razman, M. D. Morecroft, C. Nytech, A. Oliveira, G. R. Parker, S. Pulla, R. PUNCHI-Manage, H. Romero, W. Sang, J. Schurman, S. H. Su, R. Sukumar, I. F. Sun, H. S. Suresh, S. Tan, D. Thomas, S. Thomas, J. Thompson, R. Valencia, A. Vicentini, A. Wolf, S. Yap, W. Ye, Z. Yuan, J. Zimmerman. 2013. Scale-dependent relationships between species richness and ecosystem function in forests. *Journal of Ecology* 101: 1214-1224. doi: <http://dx.doi.org/10.1111/1365-2745.12132>
- Erickson, D. L., F. A. Jones, N. G. Swenson, N. Pei, N. A. Bourg, W. Chen, S. J. Davies, X-J. Ge, Z. Hao, C. L. Huang, R. W. Howe, C-L. Huang, A. J. Larson, S. K. Y. Lum, J. A. Lutz, K. Ma, M. Meegaskumbura, X. Mi, J. D. Parker, I. F. Sun, S. J. Wright, A. T. Wolf, W. Ye, D. Xing, J. K. Zimmerman, W. J. Kress. 2014. Comparative evolutionary diversity and phylogenetic structure across multiple forest dynamics plots: a mega-phylogeny approach. *Frontiers in Genetics*. doi: <http://dx.doi.org/10.3389/fgene.2014.00358>
- Gabrielson, A. T., A. J. Larson, J. A. Lutz, and J. J. Reardon. 2012. Biomass and burning characteristics of sugar pine cones. *Fire Ecology* 8(3): 58-70.
- Lutz, J. A., A. J. Larson, J. A. Freund, M. E. Swanson, K. J. Bible. 2013. The importance of large-diameter trees to forest structural heterogeneity. *PLOS ONE* 8(12): e82784. doi: <http://dx.plos.org/10.1371/journal.pone.0082784>
- Lutz, J. A. 2015. The evolution of long-term data for forestry: large temperate research plots in an era of global change. *Northwest Science* 89(3): 255-269. doi: <http://dx.doi.org/10.3955/046.089.0306>

- Lutz, J. A., A. J. Larson, M. E. Swanson, J. A. Freund. 2012. Ecological importance of large-diameter trees in a temperate mixed-conifer forest. *PLoS ONE* 7(5): e36131. doi: <http://dx.doi.org/10.1371/journal.pone.0036131>
- Lutz, J. A., K. A. Schwindt, T. J. Furniss, J. A. Freund, M. E. Swanson, K. I. Hogan, G. E. Kenagy, and A. J. Larson. 2014. Community composition and allometry of *Leucothoe davisiae*, *Cornus sericea*, and *Chrysolepis sempervirens*. *Canadian Journal of Forest Research* 44(6): 677-683. doi: <http://dx.doi.org/10.1139/cjfr-2013-0524>
- Michel, L. A., D. J. Peppe, J. A. Lutz, S. G. Driese, H. M. Dunsworth, W. E. H. Harcourt-Smith, W. H. Horner, T. Lehmann, S. Nightingale, and K. P. McNulty. 2014. Remnants of an ancient forest provide ecological context for Early Miocene fossil apes. *Nature Communications* 5: 3236. doi: <http://dx.doi.org/10.1038/ncomms4236>
- Raleigh, M. S., K. Rittger, C. E. Moore, B. Henn, J. A. Lutz, and J. D. Lundquist. 2013. Ground-based testing of MODIS fractional snow cover in subalpine meadows and forests of the Sierra Nevada. *Remote Sensing of Environment* 128: 44-57. doi: <http://dx.doi.org/10.1016/j.rse.2012.09.016>
- Stephens, S. L., M. A. Finney, and H. Schantz. 2004. Bulk density and fuel loads of ponderosa pine and white fir forest floors: impacts of leaf morphology. *Northwest Science* 78(2): 93-100.